Gyrotropic Resonances in Afterglow Plasmas*

H. J. SCHMITT, G. MELTZ, AND P. J. FREYHEIT
Sperry Rand Research Center, Sudbury, Masschusetts
(Received 16 December 1964; revised manuscript received 2 April 1965)

Resonances are observed in the reflection of radio waves from a decaying plasma column in an axial magnetic field. They are seen by monitoring the reflected signal as a function of time in the afterglow with the frequency and magnetic field held constant. When viewed collectively as a function of field strength, these observations trace the transition between Tonks-Dattner electroacoustic modes in the plasma sheath and gyrotropic longitudinal modes in the plasma core. At weak fields, the resonances are slightly displaced towards lower densities (later in the afterglow) and damped near each harmonic of the electron cyclotron frequency. As the field is increased beyond a threshold value, each mode is sharply shifted towards lower densities and rapidly attenuated until it reappears at a higher electron density, i.e., earlier in the afterglow. The observed phenomena are explained on the basis of the linearized Vlasov equation for an inhomogeneous plasma. As in the theory of Tonks-Dattner resonances, density gradients play a fundamental role in determining the resonance spectrum. Their effect is reflected in an approximate dispersion relation derived from the Vlasov equation by a perturbation approach. The resonance conditions are determined from this relation in the case of weak fields, or from the Bernstein relation in the case of stronger fields, by introducing a locally varying phase constant and applying a selection rule derived from the WKB approximation. Although the agreement between measured values and predicted results is only semiquantitative, the major trends are in accord with the theory. In particular, the analysis points out that the role of density gradients in establishing the transition between the weak- and strong-field limits is largely governed by the relative size of the Larmor radius compared with the effective scale length of the gradient.

I. INTRODUCTION

THE comparatively slow speed of electroacoustic waves gives rise to an interesting class of resonance phenomena in bounded, inhomogeneous plasmas of small extent. These phenomena are associated with longitudinal standing waves which, in the absence of a magnetic field, are confined to a narrow volume near the plasma boundary. The principal purpose of this paper is to examine the influence of an axial magnetic field on this class of resonances, the so-called Tonks-Dattner resonances, and thereby discuss electroacoustic-wave propagation across a magnetic field in an inhomogeneous plasma. A bounded plasma also exhibits another, quite distinct, class of resonances which arise from collective oscillations of the electron gas as a whole, independent of the random motion of the particles. These resonances, in contrast to the class studied in this paper, are independent of the electron temperature.

Resonant phenomena in bounded plasmas have been the subject of many experimental and theoretical investigations. Prominent among these are the early observations of Tonks,[1] the detailed experiments of Dattner,[2] and the definitive theoretical work of Parker, Nickel, and Gould,[3] supplemented by the work of Crawford and Kino,[4] Vandenplas and Messian,[5] Weissglas,[6] Hoh,[7] and others.[8] Tonks,[1] Dattner,[2] and others[9–11] also noted the effect of a magnetic field, but because of their experimental conditions they could not observe its influence on the entire spectrum of resonances.

The electroacoustic resonances discussed above occur in an underdense region of the plasma; that is, where the excitation frequency ω exceeds the local plasma frequency ω_p. The overdense region of the plasma will also support resonances but only in the presence of a sufficiently strong magnetic field. These were first seen in absorption by Buchsbaum and Hasegawa[12] and earlier, in emission, by Mitani, Kubo, and Tanaka.[13] Several other observations of these resonances were reported by Crawford, Kino, and Weiss[14] and Harp.[15]

The observations reported herein, when viewed collectively as a function of field strength, trace the transition between Tonks-Dattner resonances in the plasma sheath and gyrotropic longitudinal modes in the plasma core. Experimentally, the resonances are seen by monitoring the reflection of radio waves from a plasma column as a function of time in the afterglow of a pulsed discharge, or equivalently, as a function of electron density, while the frequency and magnetic field are held constant.

* The research reported in this paper was sponsored in part by the Air Force Cambridge Research Laboratories, Office of Aerospace Research, under Contract No. AF 19(628)-4183.

[1] L. Tonks, Phys. Rev. **37**, 1458 (1931).
[2] A. Dattner, Ericsson Technics **2**, 310 (1957).
[3] J. V. Parker, J. C. Nickel, and R. W. Gould, Phys. Fluids **7**, 1489 (1964).
[4] F. W. Crawford and G. S. Kino, *Proceedings of the Sixth International Conference on Ionization Phenomena in Gases* (Paris, 1963) Vol. III, p. 51; also *Microwave Laboratory Report No. 1045*, Stanford University, Stanford, California, 1963 (unpublished).
[5] P. E. Vandenplas and A. M. Messian, *Proceedings of the Sixth International Conference on Ionization Phenomena in Gases* (Paris, 1963) Vol. III, p. 33.
[6] P. Weissglas, Phys. Rev. Letters **10**, 206 (1963).
[7] F. C. Hoh, Phys. Rev. **133**, A1016 (1964).
[8] (a) J. A. Fejer, Phys. Fluids **7**, 439 (1964); (b) H. J. Schmitt, Appl. Phys. Letters **4**, 111 (1964).
[9] A. M. Messian and P. E. Vandenplas, Physica **28**, 537 (1962).
[10] F. W. Crawford and G. S. Kino, Phys. Letters **4**, 240 (1963).
[11] J. C. Nickel, J. V. Parker, and R. W. Gould, Bull. Am. Phys. Soc. **10**, 211 (1965).
[12] S. J. Buchsbaum and A. Hasegawa, Phys. Rev. Letters **12**, 685 (1964).
[13] K. Mitani, H. Kubo, and S. Tanaka, J. Phys. Soc. Japan **19**, 211 (1964).
[14] F. W. Crawford, G. S. Kino, and H. H. Weiss, Phys. Rev. Letters **13**, 229 (1964).
[15] R. S. Harp, Appl. Phys. Letters **6**, 51 (1965).

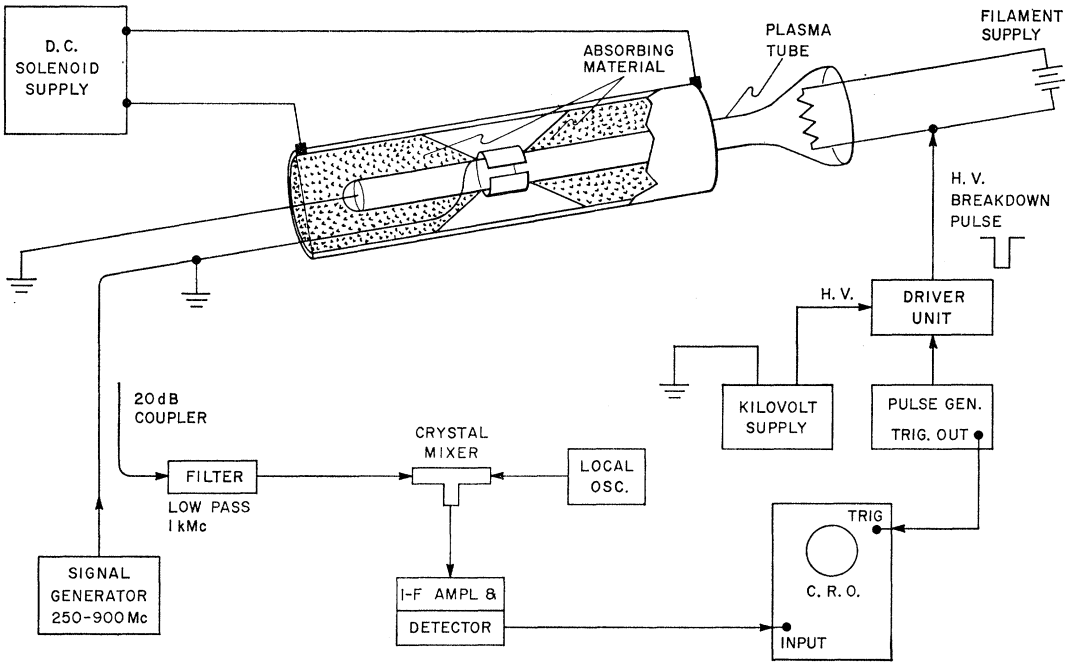

FIG. 1. Schematic diagram of the experiment. Resonances are excited in the 3-cm-diam discharge tube by a strip-line capacitor.

For each value of the harmonic number ω/Ω (where Ω is the electron gyrofrequency), one observes a set of resonances which are attributable to the several electroacoustic modes that may be excited within the plasma. At weak fields or large harmonic numbers, the resonances are displaced towards lower densities and undergo small perturbations and damping near each harmonic. As the field is increased beyond some threshold value, each mode is sharply shifted towards lower densities and rapidly attenuated until it reappears at a higher electron density. Thus, in a sense, the resonances "split" as the field is increased.

Our explanation of the observed phenomena is based on the linearized Vlasov equation for an inhomogeneous plasma. The important effect of density gradients is retained by introducing a locally varying phase constant which is obtained from an approximate dispersion relation. Because of the mathematical complexity of the Vlasov equation, it is not possible to obtain a single dispersion relation which is applicable over the entire range of magnetic-field strengths. Rather, we derive the strong- and weak-magnetic-field limits and, through a perturbation approach, extend these results to intermediate values of the applied field.

The paper is organized into three major sections with the details of the experiment described in Sec. II. The experimental results and their theoretical interpretation are grouped into the remaining sections according to whether the resonances occur in an underdense (Sec. III) or overdense (Sec. IV) regime of the afterglow.

II. EXPERIMENTAL SYSTEM

Resonances are excited in a cylindrical discharge tube by a short section of open-ended strip line, spaced 3 mm from the wall and nearly encircling a narrow section of the tube. The discharge is centered within the uniform field region of a long solenoid and the resonances are observed by monitoring the reflected power as a function of time in the afterglow, or equivalently, as a function of electron density, while the magnetic field is held constant (Fig. 1). A typical measurement in the absence of a magnetic field is shown in Fig. 2. Each absorption dip in the trace of the reflected signal corresponds to the excitation of a new electroacoustic eigenmode.[16] When an axial magnetic field is applied, each resonance is shifted in time and changed in amplitude.

The results which are presented in this paper were obtained from measurements in neon at 0.3 and 0.1 Torr. Similar measurements, also in neon, were made from 0.01 to 3 Torr and at a number of frequencies between 200 and 800 Mc/sec. Within these ranges, the observed

[16] In our experiment, the so-called "main resonance" or cold-plasma dipole resonance (Ref. 3) cannot be observed unless metallic chokes are placed along the discharge tube on both sides of the strip line. In a low-temperature afterglow, the "main resonance" lies between the first and second electroacoustic resonances, its exact position depending slightly on the spacing between the chokes. For the localized excitation provided by a narrow strip line, the discrete cold-plasma resonance degenerates into an electromagnetic surface wave that propagates along the plasma column. This wave is only observed as a resonance if reflecting surfaces are introduced to create axial standing waves. These spurious resonances are eliminated in our experiment by tightly packing absorbing material about the ends of the tube.

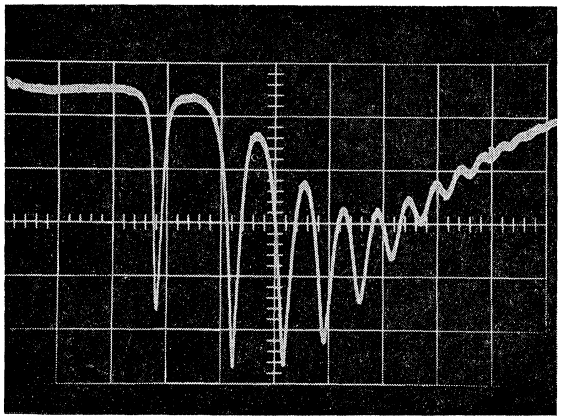

FIG. 2. Tonks-Dattner resonances observed in reflection in the afterglow of a neon discharge at 0.3 Torr.

phenomena are virtually independent of the gas pressure and frequency of excitation. Observations in tubes of different diameter and in other noble gases also gave substantially similar results.

The instantaneous electron density in the discharge has been determined as a function of time in the afterglow by two independent methods. The first method relies on the onset of plasma absorption which occurs when the excitation frequency is approximately equal to the peak hybrid frequency $(\omega_{p0}^2+\Omega^2)^{1/2}$, where ω_{p0} is the peak angular plasma frequency in the center of the tube. The onset is observable as a sharp bend in the trace of the reflected power. Measurements of the density decay for weak magnetic fields ($B<70$ G) and at late times in the afterglow ($t>2.5$ msec) indicate a diffusion-dominated loss mechanism (Fig. 3). A diffusion-dominated decay is expected under these conditions on the basis of a comparison of the time scales for recombination processes and radial ambipolar diffusion losses. The density decay also follows an exponential law for stronger magnetic fields ($B=140$ G), but only at much later times in the afterglow.

The second method of determining the peak density relies on an evaluation of the Tonks-Dattner resonance spectrum at different frequencies (cf. Appendix). The peak plasma frequency as inferred from the resonance positions at 3 different signal frequencies is plotted in Fig. 3. Over the range where the density decay is exponential, close agreement is obtained with data determined from the onset of plasma absorption. In the earlier part of the afterglow, a slight disagreement arises due to a difference in the density profile or a higher electron temperature than assumed for the calculations ($T_e=300$°K). We conclude that the afterglow is diffusion controlled and substantially in thermal equilibrium with the neutral gas, except for small deviations in the time regime of the first resonance at 250 Mc/sec.

A plot of the measured diffusion constant as a function of magnetic field strength is shown in Fig. 4. In the absence of a magnetic field, the measured value is in fair agreement with the result of Biondi,[17] and decreases insignificantly over the range of field strengths used in our experiment. These results are substantially in accord with the theory of classical collisional diffusion[18] across a magnetic field.

III. RESONANT MODES IN AN UNDERDENSE PLASMA

A. Experimental Results

A compilation of experimental results observed in neon at 0.3 Torr and at 250 Mc/sec shows the shift and subsequent splitting of several resonant modes as the magnetic field is increased (Fig. 5). Note that the slight monotonic shift at weak fields is accompanied by small perturbations near each harmonic. As the field is increased beyond some threshold value and the next harmonic approached, each mode is sharply shifted towards later times in the afterglow, i.e., towards lower densities, and rapidly attenuated until it reappears at an earlier time, i.e., at a higher density. The onset of these effects for higher order resonances occurs at successively lower magnetic-field strengths.

A repetitive pattern occurs in each strip between successive harmonics beyond the threshold. This pattern is observed under conditions where many Larmor orbits fit within the characteristic length of the plasma resonator. For weak magnetic fields, the pattern resembles previous observations by Messian and Vandenplas.[9] However, the clarity of our observations, which is primarily ascribable to the typically low electron temperatures and small collison rates of afterglow plasmas, allows us to extend these measurements to stronger fields.

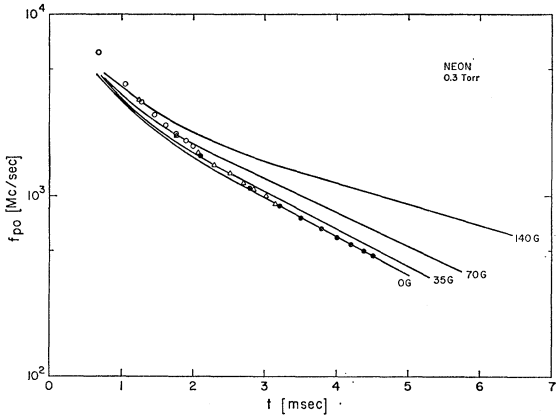

FIG. 3. Peak plasma frequency as a function of time in the afterglow of neon at 0.3 Torr. Solid curves for different magnetic fields are obtained from measurement of absorption onset. Discrete points are obtained from Tonks-Dattner resonances in the absence of a magnetic field at three frequencies (● 250 Mc/sec, △ 400 Mc/sec, ○ 600 Mc/sec). The density decay is exponential beyond the range shown.

[17] M. A. Biondi, Phys. Rev. **79**, 733 (1950).

[18] F. Boeschoten, J. Nucl. Energy Pt. C **6**, 344 (1964). F. C. Hoh, Rev. Mod. Phys. **34**, 267 (1962).

B. Theoretical Discussion

Our theoretical interpretation is based on an approximate solution of the linearized Vlasov equation for wave motion perpendicular to a magnetic field in a quasihomogeneous plasma. In our model, the effect of density gradients is retained to lowest order by introducing a locally varying wave number as a perturbation to the solution for a uniform plasma. For time harmonic disturbances and using conventional subscript notation to distinguish perturbation and equilibrium quantities

$$(j\omega+\mathbf{v}\cdot\nabla_r)f_1-[(e/m)\mathbf{E}_0+\Omega(\mathbf{v}\times\hat{z})]\cdot\nabla_v f_1 = (e/m)\mathbf{E}_1\cdot\nabla_v f_0. \quad (1)$$

The parameters are the electron gyrofrequency Ω, the average thermal velocity v_T associated with f_0,[19] and $\mathbf{E}_0$ the zeroth-order electric field required to maintain a locally varying electron density $n(r)$. It is somewhat difficult to establish precisely the magnitude and direction of $\mathbf{E}_0$ in the presence of axial magnetic fields. Classically,

$$\mathbf{E}_0=-\frac{\nabla_r n}{n}\frac{D_{e\perp}-D_{i\perp}}{\mu_{e\perp}+\mu_{i\perp}}, \quad (2)$$

if the principal loss of particles is by collisional diffusion across the magnetic field.[18] The ambipolar diffusion coefficient across the field is determined by

$$D_{a\perp}=\frac{D_{e\perp}\mu_{i\perp}+D_{i\perp}\mu_{e\perp}}{\mu_{e\perp}+\mu_{i\perp}}, \quad (3)$$

where $\mu_{e\perp,i\perp}$ are the mobilities and diffusion coefficients for electron and ion motion perpendicular to the magnetic field. Combining Eqs. (2) and (3), we obtain

$$\mathbf{E}_0=-(\nabla_r n/n)[(D_{a\perp}-D_{i\perp})/\mu_{i\perp}]. \quad (4)$$

Within the range of magnetic fields used in our experiment, $D_{a\perp}$ is almost unchanged. Consequently, if the effect of the magnetic field on ion motion is also negligible,[20] then it is reasonable to expect that the unperturbed electric field is substantially the same as the value in the absence of an impressed magnetic field

$$\mathbf{E}_0\simeq-(m/e)(KT/m)(\nabla_r n/n). \quad (5)$$

Using this estimate for the zeroth-order electric field, Eq. (1) becomes

$$(j\omega+\mathbf{v}\cdot\nabla_r)f_1+\Omega v_T[\rho\nabla_r n/n+(1/v_T)\hat{z}\times\mathbf{v}]\cdot\nabla_v f_1 = (e/m)\mathbf{E}_1\cdot\nabla_v f_0. \quad (6)$$

It can be seen that the relative magnitude of the acceleration terms[21] in the second bracket depends on the ratio of the Larmor radius $\rho=v_T/\Omega$ to the effective scale length of the gradient $(\nabla_r n/n)^{-1}$. An estimate of this ratio can be obtained by introducing an appropriate average value l for $(\nabla_r n/n)^{-1}$,[22] i.e.,

$$\rho\langle\nabla_r n/n\rangle=\rho/l.$$

For a very weak magnetic field, $\rho\langle\nabla_r n/n\rangle$ is large and, provided that the gradient is gradual in terms of Debye lengths ($\lambda_D\langle\nabla_r n/n\rangle\ll 1$), Eq. (6) yields the Bohm-Gross dispersion relation. A better approximation which retains lowest order magnetic-field effects follows from the moment equations[7] or from the weak-magnetic-field–low-temperature limit given by Bernstein[23]:

$$k^2=k_0^2\equiv\{\omega^2-[\omega_p^2(x)+\Omega^2]\}/3v_T^2. \quad (7)$$

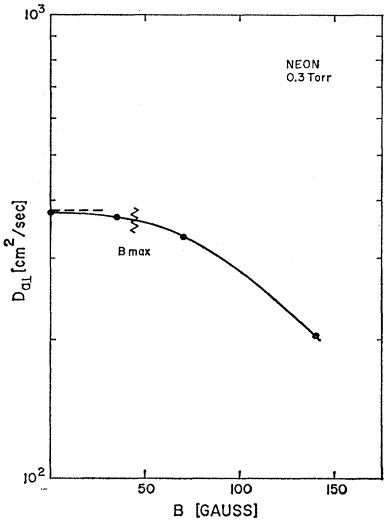

FIG. 4. Measured coefficient of ambipolar diffusion across the magnetic field as a function of field strength. Dashed line shows zero-field value given by Biondi (Ref. 17).

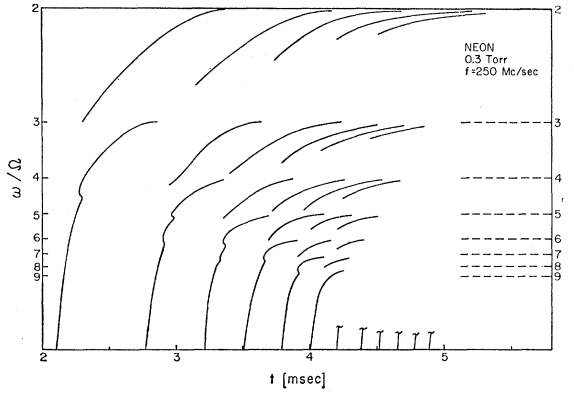

FIG. 5. Radial electron plasma-wave resonances in cylindrical afterglow plasma as a function of time in the afterglow and axial magnetic field. Modes beyond the sixth, shown only for weak fields, have also been traced through the harmonic where splitting first occurs.

[19] The equilibrium distribution function f_0 is assumed to be Maxwellian in velocity space.

[20] The mean free path of ions is small compared to their Larmor radius and the tube diameter.

[21] For an order-of-magnitude comparison, it is assumed that there are few particles with velocities much in excess of the average thermal velocity.

[22] The length l is computed by averaging $\nabla_r n/n$ over the region in which wave propagation takes place. For a fixed value of the magnetic-field strength and a constant frequency, l increases with mode number. Higher order modes extend deeper into the plasma and consequently are associated with smaller average gradients or larger values of l.

[23] I. B. Bernstein, Phys. Rev. **109**, 10 (1958).

Clearly, Eq. (7) cannot account for the observed perturbations near harmonics. It does, however, predict the gradual shift of the zero-field Tonks-Dattner resonance to lower densities as the magnetic field is increased.

For strong magnetic fields, $\rho\langle n'/n\rangle \ll 1$. In this limit, provided that that $\lambda_D\langle \nabla_r n/n\rangle \ll 1$, Eq. (6) yields a dispersion equation of the form previously derived by Bernstein:

$$\Lambda = \frac{\omega_p^2(x)}{\Omega^2} \sum_{p=1}^{\infty} \frac{2p^2}{(\omega/\Omega)^2 - p^2} I_p(\Lambda) e^{-\Lambda}, \tag{8}$$

where $\Lambda \equiv (k\rho)^2$ and k is the local wave number. Although this relation exhibits a periodicity with increasing harmonic number p and accurately predicts phenomena for strong magnetic fields and high-order modes, it cannot account for the observed monotonic shift at weak fields. Note that in deriving these relations we have assumed, for simplicity, a slab model of the cylindrical plasma.[24]

In the transition region between the two previous limits, both the Lorentz force and the electric force associated with the density gradient must be retained. Proceeding in the spirit of a perturbation analysis, we attempt to estimate the interaction term $v_T\rho(\nabla n/n)(\partial f/\partial v_x)$ for weak magnetic fields. Differentiating Eq. (6) with respect to v_x, neglecting both the electric force and the Lorentz force terms in the second bracket, and replacing $\nabla_r f_1$ by $j\bar{k}f_1$ where $\bar{k}$ is the propagation constant in an isotropic plasma, we obtain the following estimate

$$\frac{\partial f_1}{\partial v_x} \sim \frac{(e/m)E_x(\partial^2/\partial v_x^2)f_0}{j\omega(1-\bar{k}v_x/\omega)} + \frac{j\bar{k}f_1}{j\omega(1-\bar{k}v_x/\omega)} \sim \frac{\bar{k}}{\omega} f_1. \tag{9}$$

Thus, to the order of approximation where $\bar{k}v_x/\omega \ll 1$, we have $\partial f_1/\partial v_x \sim (\bar{k}/\omega)f_1$. For weak magnetic fields, this estimate is improved by replacing $\bar{k}$ by k_0 defined in Eq. (7).

Substituting this result into Eq. (6), we obtain the following approximate form of the kinetic equation

$$\left[j\left(\frac{\omega}{\Omega} - j\frac{v_T k_0}{\omega}\rho\frac{\nabla n}{n}\right) + \frac{\mathbf{v}\cdot\nabla}{\Omega}\right] f_1 + (\hat{z}\times\mathbf{v})\cdot\nabla_v f_1 \simeq \frac{e}{m\Omega}\mathbf{E}\cdot\nabla_v f_0. \tag{10}$$

Note that this approximation has in effect introduced a complex frequency or damping which is to be associated with the interaction between pressure gradient and Lorentz forces. One recalls that in a homogeneous medium collisionless damping does not occur for propagation across the magnetic field; however, it does appear for propagation at an arbitrarily small angle to the field.[25] Moreover, one cannot obtain the Bohm-Gross result from the general form of the Bernstein dispersion results without retaining this damping in the limiting procedure. Mathematically, the same problem appears in treating the influence of gradients.

Using Poisson's equation in (10) and formally integrating the result, we obtain the following

$$-E_{x1}'' \simeq \frac{4\pi e^2}{mv_T^2}\left\{j\tilde{\omega}/\Omega \int_0^{\infty} \exp\left[-\frac{j\tilde{\omega}}{\Omega}y + \rho^2(1-\cos y)\frac{\partial^2}{\partial x^2}\right]dy - 1\right\} nE_{x1} \tag{11}$$

where $\tilde{\omega}/\Omega$ is a complex frequency defined by $\omega/\Omega - j(v_T k_0/\omega)\rho\langle n'/n\rangle$. Note that the damping or imaginary part of $\tilde{\omega}$ increases with $\rho\langle n'/n\rangle$. The derivation of Eq. (11) is identical to that given by Bernstein with the exception that ω is replaced by $\tilde{\omega}$ and $-k^2$ by $\partial^2/\partial x^2$.

For low temperature and weak magnetic fields, the major contribution to the integral arises from the vicinity of $y=0$ where the attenuation term contained in the complex frequency is negligible. Replacing $\partial^2/\partial x^2$ with $-k^2$, one obtains to lowest order in the expansion parameter $k\rho$

$$k^2\rho^2 = \frac{\omega_p^2}{\omega^2}\left\{k^2\rho^2\left(1+\frac{\Omega^2}{\omega^2}\right) + 3k^4\rho^4\frac{\Omega^2}{\omega^2}\cdots\right\} \tag{12}$$

or

$$k = k_0 = \left(\frac{\omega^2 - (\omega_p^2+\Omega^2)}{3v_T^2}\right)^{1/2},$$

our previous result.

The major correction to k_0 will arise from the sequence of relative maxima in the integrand which occur near $y = 2\pi p$, $p = 1,2,\cdots$. Because of the attenuation term in $\tilde{\omega}/\Omega$, these contributions decrease in amplitude with increasing values of the harmonic number p. We proceed by replacing $\partial/\partial x$ by jk_0, an approximation which is valid for weak magnetic fields, changing variables to $z = 2\pi p - y$ and developing $1-\cos y$ to second order in z. The contribution of each maximum is evaluated separately by bilaterally extending the range of integration to infinity. The sum of these integrals yields the following dispersion relation:

$$k \simeq k_0\left\{1 - \left(\frac{1}{6}\right)2^{1/4}\pi^{1/2}\left(\frac{\omega}{\Omega}\right)^{5/2} \times \left(\frac{\omega}{k_0 v_T}\right)^{5/2} \exp\left[-\frac{1}{2\sqrt{2}}\left(\frac{\omega}{\Omega}\right)\left(\frac{\omega}{k_0 v_T}\right)\right] \times \frac{\exp[-j(2\pi\tilde{\omega}/\Omega - \pi/2)]}{1-\exp(-j2\pi\tilde{\omega}/\Omega)}\right\}. \tag{13}$$

[24] If the resonances are confined to a narrow underdense region near the wall, as they are for weak and moderate magnetic fields, then the dominant modes are mainly radial and dipolar. Under these conditions, it is unlikely that quadrupole or higher order multipole modes would be observed since the eigenvalues of these modes nearly coalesce with those of the dipole mode. Moreover, since the width of the resonance region is small compared to the radius of the tube, we may neglect the curvature and use a plane-layer model.

Note that the imaginary part of k accounts for the attenuation of the longitudinal waves. It is strongest where ω/Ω is an integer, hence, exactly at a harmonic as observed experimentally. Within the limits of validity for Eq. (13), the attenuation also becomes more pronounced with increased magnetic field. In view of the perturbation procedure, the range of validity is limited to the region where $\rho\langle n'/n\rangle > 1$.

Using these results, we can estimate the resonant frequency of any order mode by applying a selection rule derived from the WKB approximation in conjunction with the locally varying wavenumber $k=k(x)$. In the spirit of this technique, a resonance condition is established by equating the total phase between reflection points to a rational multiple of π determined by the reflection conditions of the particular mode in question.[26] Since the density profile is known, the variation of k within the plasma, for a fixed harmonic ratio ω/Ω, can be inferred from dispersion curves which display $k/k_T \equiv k\omega/v_T$ as a function of ω_p/ω.

A representative set of curves for the propagation constant calculated from the Bernstein relation is shown in Fig. 6. Numerical computations for higher harmonic numbers indicate a periodicity with harmonic ratio in accord with the repetitive pattern in the measured resonant structure for $\rho\langle n'/n\rangle \ll 1$, Fig. 5. Note that the curves intersect the ordinate at a point determined by the hybrid resonance condition $\omega^2=\omega_p{}^2+\Omega^2$ and continue to an asymptotic wavenumber as $\omega_p/\omega \to \infty$.

With moderate density gradients, undamped waves can propagate in a region bounded by a surface where the angular rf equals the hybrid frequency and a surface with a local-plasma frequency corresponding to the value associated with the minimum in the curves of Fig. 6. For this electron density, the group velocity vanishes. For lower densities, the propagation constant becomes complex resulting in a damping of electron acoustic waves. (The real part of the complex wavenumber is shown by a thin, solid line.) For magnetic fields near the harmonic, e.g., $\omega/\Omega \sim 2.05$, 3.05 or 4.05, etc., this damping may be small due to the narrow space in which the density is low, and resonances may be set up between the wall and a surface within the plasma where the hybrid frequency is equal to the applied frequency. The propagation constant for such modes is always smaller, and hence the wavelength longer, than in an isotropic plasma of equal density. This leads to a smaller phase integral and a resonance at a lower peak density than for the corresponding mode in an isotropic plasma. In the limit $\omega/\Omega \to p$, the wavelengths become extremely large, and all resonances vanish. As the magnetic field is decreased from its value near an exact harmonic, damping becomes stronger and ultimately prevents observation of the resonances.

On the basis of this model, the position of the observed

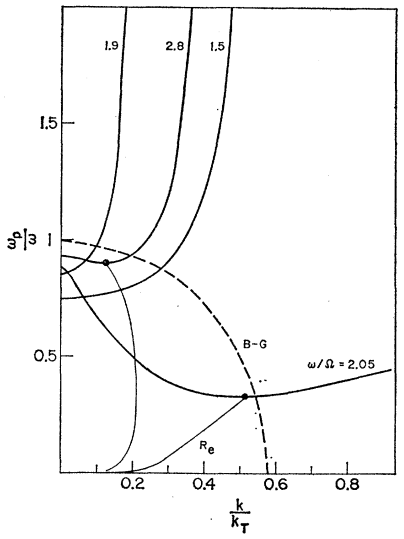

FIG. 6. Dispersion curves for propagation normal to the magnetic field. Dashed line (B-G) is the zero-field limit and thin solid lines (Re) are the real parts of the complex extensions of the Bernstein modes. The wave number k is normalized by ω/v_T, where v_T is the electron thermal velocity.

resonances in the cylindrical plasma column may be predicted in a region where $\rho\langle n'/n\rangle \ll 1$. The results are shown in Fig. 7 by the thin solid lines and thin dashed extensions, the latter corresponding to highly damped solutions. Although the agreement is semiqualitative, the major trends are in agreement with the measurements, indicated as heavy lines. The theoretical result for the first resonance is displaced from the experimental value by a fixed amount related to the difference between the peak density obtained from the onset of plasma absorption and the value inferred from measurements of the Tonks-Dattner resonances. (See Figs. 3 and 5.) The value obtained from the onset of cold-plasma absorption has been used in the computation of the predicted first-order mode. In the case of higher order resonances, no discrepancy occurred between the independently measured values of the peak density.

The dispersion curve for the weak magnetic field limit $\rho\langle n'/n\rangle \gg 1$ is also shown in Fig. 6 for comparison. The predicted resonance pattern obtained in this case (thin solid lines in Fig. 7) correlates with the gross shift in the resonant frequency but does not account for the observed major splitting or minor perturbations near harmonics. Corrections to this result, obtained from Eq. (13) in conjunction with the WKB procedure, are shown for the first resonant mode ($m=0$) by a thin solid curve with rapidly damped fluctuations which are interrupted by dashed sections near a harmonic to indicate attenuation. For purposes of this calculation, we use an average value for k_0 and $\rho\langle n'/n\rangle$ in the perturbation term in Eq. (13). Explicitly,

$$\left\langle \frac{k_0 v_T}{\omega} \right\rangle \equiv \frac{v_T}{\omega} \int_{r_0}^{a} \frac{k_0}{a-r_0} dr \simeq 0.409(1-(\Omega/\omega)^2)^{1/2}, \quad (14)$$

where a is the radius of the tube and r_0 the interior turning point $k(r_0)=0$. A more detailed numerical calculation which also considers the locally varying

[25] I. B. Bernstein Ref. 23, p. 16.

[26] A classical turning point occurs at the interior surface where $\omega^2-(\omega_p{}^2+\Omega^2)=0$; specular reflection is assumed at the wall.

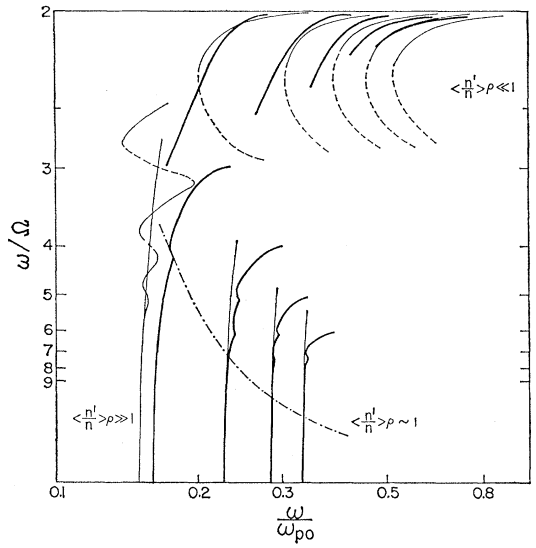

FIG. 7. Radial electron plasma-wave resonances in cylindrical plasma column as a function of peak plasma frequency and magnetic field. Heavy lines are experimental results from Fig. 5. Theoretical results are shown as thin solid lines for strong ($\langle n'/n\rangle\rho\ll 1$) and weak magnetic fields ($\langle n'/n\rangle\rho\gg 1$). Dashed continuations correspond to damped resonances. Resonant positions in transition region are shown as a thin oscillating curve for first resonant mode.

nature of these parameters in the perturbation term is probably not justified in view of the approximate nature of the dispersion relation. Even so, fair agreement with the experiment is obtained and serves to suggest the role of density gradients in establishing the transition between the two regions. Apparently, the main effect of a gradient is to dampen the pronounced resonance phenomenon near harmonics of the electron cyclotron frequency. The transition from one extreme of the dispersion relation to the other extreme is gradual and is determined in order of magnitude by the size of the scale factor $\rho\langle n'/n\rangle$.

Wave propagation in both the strong- and weak-magnetic-field limits occurs in a region between the wall and an inner surface where the applied frequency equals the local hybrid frequency. The average value of the scale ratio $\rho\langle n'/n\rangle$ within this region is obtained from from Eq. (A3) of the Appendix and is given by

$$\rho\left\langle\frac{n'}{n}\right\rangle\sim 2\alpha J_1(\alpha)\left[\frac{\omega_{p0}^2}{\omega^2-\Omega^2}+\frac{1}{3}\frac{J_2(\alpha)}{J_1^2(\alpha)}\right]\frac{v_T}{a\omega}\left(\frac{\omega}{\Omega}\right) \quad (15)$$

where $\alpha=2.405$ and ω_{p0} is the peak density at the center of the discharge. The dashed-dotted line in Fig. 7 indicates where this ratio is equal to unity. This curve roughly coincides with the onset of observable perturbations in the mode positions. In lieu of the frequency ratio ω/ω_{p0}, the mode number of Tonks-Dattner resonances for weak magnetic fields may be introduced [see Appendix, Eq. (A4)]. For a fixed mode number, the scale ratio is virtually independent of the rf frequency, the electron temperature, and the tube radius. This explains the similarity of our experimental observations at different signal frequencies and gas pressures.

IV. RESONANCES IN AN OVERDENSE PLASMA

A. Experimental Results

The resonance mode pattern discussed in the previous section applied to electron waves in inhomogeneous plasmas where $(\omega_p^2(r)+\Omega^2)^{1/2}<\omega$. In a cylindrical afterglow, this is near the wall of the tube. Inspection of Fig 6 shows that real propagation constants are also possible in the overdense case, particularly if the magnetic field is slightly stronger than that corresponding to an exact harmonic value, i.e., $\omega/\Omega\sim 1.9$, 2.9, or 3.9, etc. Under these conditions, standing waves are set up in the plasma core inside the region where the local plasma frequency corresponds to the hybrid frequency. This "resonator" may extend over almost the entire plasma cross section for a high peak density. For short-wavelength phenomena, very many wavelengths fit into this space, and resonances would be extremely narrowly spaced. Resolution of individual resonances is unlikely under these conditions. However, when the peak hybrid frequency on axis is near the rf frequency, the diameter of the "resonator" is relatively small, and individual resonances in the plasma core can be resolved.

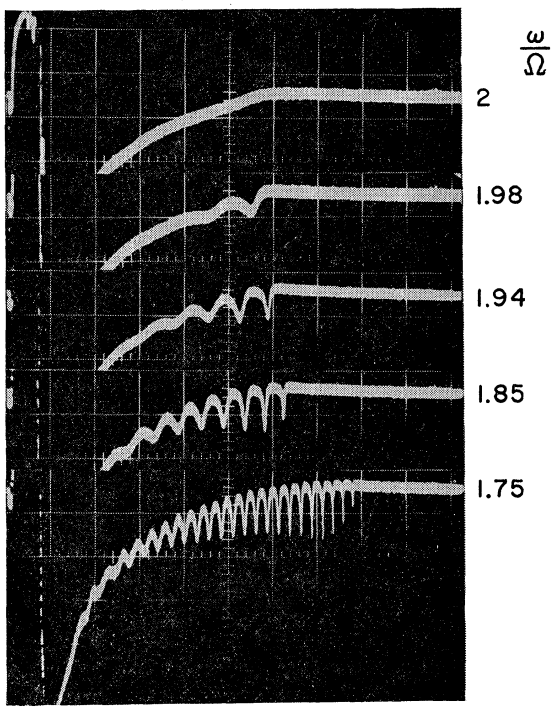

FIG. 8. Radial electron plasma-wave resonances in the core of a cylindrical plasma column for different magnetic-field strengths observed in reflection in a neon afterglow plasma, 0.02 Torr, $F=400$ Mc/sec, time scale 0.2 msec/div.

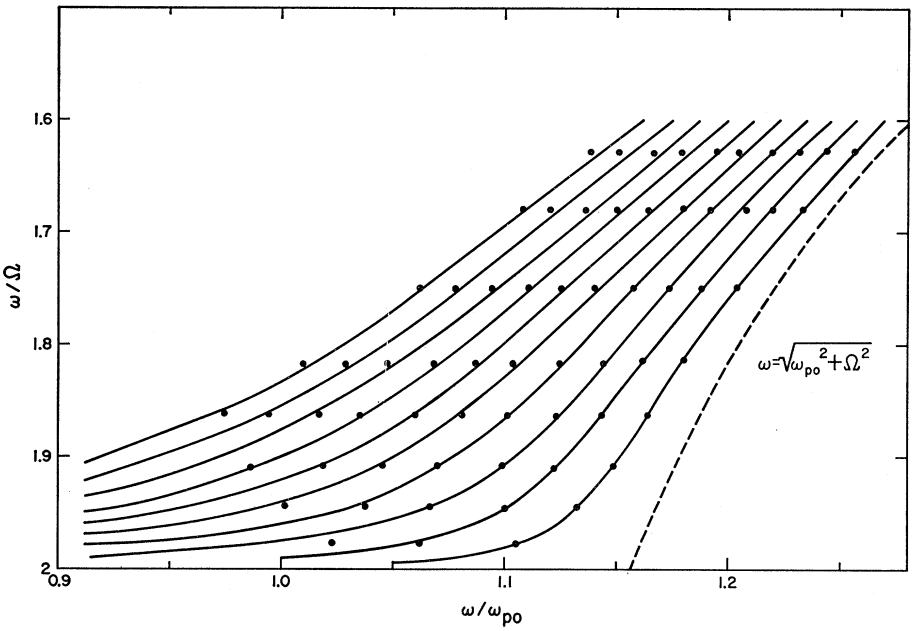

FIG. 9. Radial electron plasma-wave resonances in the core of a plasma column as a function of peak plasma frequency and axial magnetic field. (——) Resonance position for dipolar modes based on WKB approximation, $T_e=300°K$. (···) Experimental results, neon afterglow, 0.1 Torr, normalized to computed curve for lowest order resonance. Dashed line (– – –), corresponding to the hybrid resonance condition $\omega^2=\Omega^2+\omega_{p0}^2$, shows the limit of the resonant frequencies.

These resonances were first observed in noise emission[13] and subsequently studied in detail by measurements of the resonant absorption of a plasma column in a microwave cavity.[12] Related experiments have examined wave propagation between antennas immersed in a nearly uniform plasma.[14,15]

In our experiments, core resonances were observable near the second harmonic and much weaker ones near the third harmonic for gas pressures of 0.1 Torr and lower. The resonant interaction is most pronounced for low-peak plasma frequencies in the vicinity of

$$\omega_{p0}\sim(\omega^2-\Omega^2)^{1/2};$$

hence, at later times in the afterglow than the Tonks-Dattner resonances in the outer shell. Up to 35 resonaces could be resolved as a function of time in the decaying plasma column (Fig. 8).[27]

The positions of the first 10 resonances have been recorded as a function of time in the afterglow for a gas pressure of 0.1 Torr, a fixed frequency of 400 Mc/sec, and magnetic fields near the second harmonic. All resonances occur at elapsed times of more than 3 msec. A separate calibration of the electron density decay using the onset of plasma absorption again showed a diffusion-controlled loss mechanism, allowing one to relate the time scale to the instantaneous peak plasma frequency.

B. Theoretical Discussion

For the conditions of this experiment, $\rho\langle n'/n\rangle\ll 1$ and, as shown by Buchsbaum and Hasegawa,[12] the dispersion relation in the vicinity of the second harmonic may be approximated by

$$k^2=\frac{[\omega^2-(\omega_p^2(r)+\Omega^2)][\omega^2-4\Omega^2]}{3v_T^2\omega_p^2(r)}. \tag{16}$$

This form can be derived by a small temperature expansion of Eq. (8). Again using the WKB method to predict resonance conditions, one obtains[28]

$$(m+\tfrac{1}{2})\pi=\int_{r_1}^{r_2}\left(k^2(r)-\frac{(s+\frac{1}{2})^2}{r^2}\right)^{1/2}dr. \tag{17}$$

The term $\frac{1}{2}$ on the left-hand side results from combined reflection conditions at the turning points, r_1 and r_2, near the surface where $\omega_p\sim(\omega^2-\Omega^2)^{1/2}$ and near the center of the cylindrical discharge column. For dipole modes $s=\frac{1}{2}$; for quadrupole modes $s=\frac{3}{2}$. Thus, the scaling of the radial-wave equation into a one-dimensional wave equation results in a noticeable displacement of eigenmodes with higher order symmetry. The higher order modes are not observed in our experiment.[29] We have numerically integrated Eq. (17) for an afterglow profile $n=n_0J_0(\alpha r)$ at 300°K. The first 10 predicted dipolar eigenmodes are shown in Fig. 9 as a function of ω/ω_{p0} together with the theoretical limit when ω equals the peak hybrid frequency (dashed line). Experimental points are included after normalization of the last observed resonance position to the theoretical curve.

[27] It was noted in the experiment that very slight misalignments of the magnetic field with respect to the tube axis would seriously perturb the clarity and resolution of resonances.

[28] P. M. Morse and H. Feshbach, *Methods of Theoretical Physics* (McGraw-Hill Book Company, Inc., New York, 1953), Pt. II, p. 1101.

[29] Significant splitting between multipole modes takes place if the resonances arise from oscillations in the overdense plasma core (cf. discussion in Sec. IV). However, under these conditions, the effect of a multipole field can be shown to be insignificant because of the sufficiently large separation between the strip line and the effective plasma resonator (cf. Parker, Nickel, and Gould, Ref. 3).

This normalization is necessary to avoid a small scatter in the correlation of resonance sequences measured at different magnetic fields. This scatter occurs because the onset of cold-plasma absorption cannot be measured with sufficient accuracy, i.e., the scatter is comparable to the spacing of adjacent resonances as a function of ω/ω_{p0}. A comparison of the calculated curves with the experimentally observed pattern shows the fair agreement obtained. In this experiment, the electron temperature enters as a critical parameter which largely determines the spacing between consecutive resonances for any fixed magnetic field. Different measurements taken at much lower pressures and, hence, earlier in the afterglow, showed a significantly increased spacing between eigenmodes, indicating a substantially higher electron temperature. This is consistent with the slower energy relaxation rates expected for a lower gas pressure. Indeed, the observation of the separation between interior eigenmodes may offer a sensitive measurement of electron temperatures in the presence of magnetic fields.

ACKNOWLEDGMENTS

We wish to express our appreciation and indebtedness to Dr. Peter L. Auer for his contributions to this paper and for his numerous trenchant, always stimulating, discussions of the problem. The advice of Professor George Bekefi is also gratefully acknowledged. In addition, we wish to thank J. E. Morris for his technical assistance and Natalie Palk for her aid in computing the theoretical results.

APPENDIX: THE USE OF TONKS-DATTNER RESONANCES TO DETERMINE THE PEAK PLASMA DENSITY

In the absence of a magnetic field, the relation between the peak plasma frequency ω_{p0} and a particular mode m is obtained from a selection rule based on the WKB approximation and a locally varying wave number k. Explicitly,

$$(m+\tfrac{3}{4})\pi=\int_{r_0}^{a} k\,dr=\int_{r_0}^{a}\frac{(\omega^2-\omega_p^2(r))^{1/2}}{3v_T^2}\,dr, \quad (A1)$$

$$m=0, 1, \cdots,$$

where a is the radius of the tube, $v_T=(KT/m)^{1/2}$ is the thermal velocity, and r_0 is the radius at which the signal and local plasma frequencies are equal.[8b] The above relation is derived on the basis of a slab model of the narrow annular space near the wall in which plasma oscillations are excited.

The radial-electron-density profile late in a diffusion-controlled afterglow[18] is given by

$$\omega_p^2(r)=\omega_{p0}^2 J_0(\alpha r/a), \quad (A2)$$

where $\alpha=2.405$. Near the wall $x/a=(a-r)/a\ll 1$ and

$$\omega_p^2(r)\simeq\omega_{p0}^2[\alpha J_1(\alpha)x/a+(\tfrac{1}{4})\alpha^2 J_2(\alpha)(x/a)^2]. \quad (A3)$$

Evaluation of Eq. (A1) in conjunction with Eq. (A3) yields to first order in the small contribution resulting from the quadratic term of the density profile

$$(m+\tfrac{3}{4})\pi\sim\frac{2a\omega}{3\sqrt{3}v_T\alpha J_1(\alpha)}\frac{\omega^2}{\omega_{p0}^2}\left\{1-\frac{J_2(\alpha)}{5J_1^2(\alpha)}\frac{\omega^2}{\omega_{p0}^2}\right\}, \quad (A4)$$

The accuracy of this expression in determining the ratio ω/ω_{p0} is estimated to be better than $\pm 10\%$. It yields substantial agreement with calculations for a comparable profile carried out by Parker *et al.*[3] if the different electron temperature assumed in Parker's experiment is taken into account.

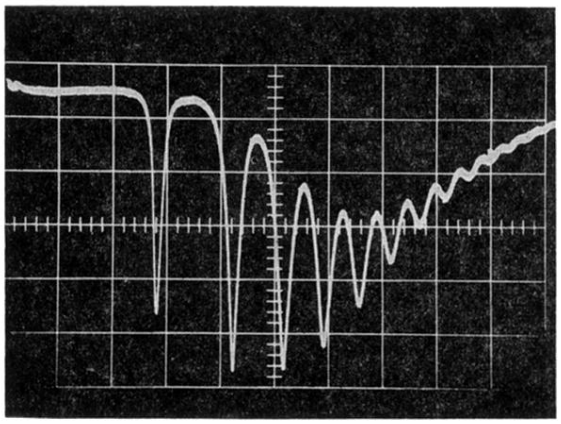

FIG. 2. Tonks-Dattner resonances observed in reflection in the afterglow of a neon discharge at 0.3 Torr.

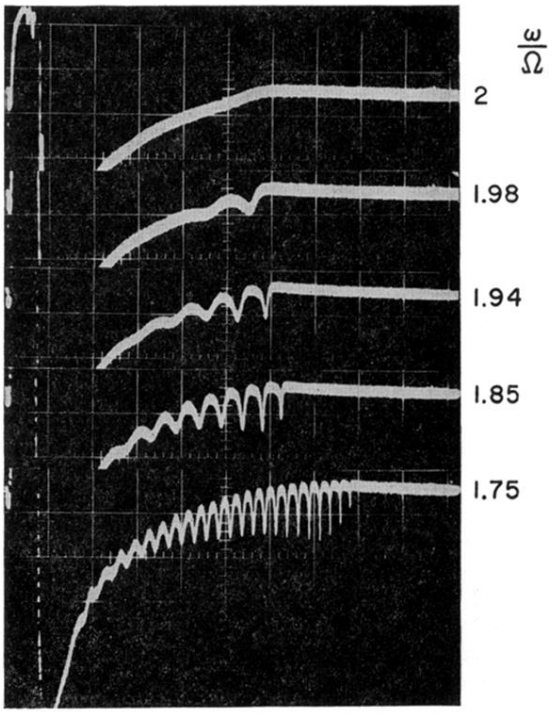

FIG. 8. Radial electron plasma-wave resonances in the core of a cylindrical plasma column for different magnetic-field strengths observed in reflection in a neon afterglow plasma, 0.02 Torr, $F=400$ Mc/sec, time scale 0.2 msec/div.